Phytopathologia Mediterranea
The international journal of the
Mediterranean Phytopathological Union

Firenze University Press
www.fupress.com/pm

Research Papers

Identification and characterization of *Aspergillus* species associated with Aspergillus vine canker of table grapes in Spain

Adnan ALI, Maela LEÓN, Mónica BERBEGAL, Josep ARMENGOL*

Instituto Agroforestal Mediterráneo, Universitat Politècnica de València, Camino de Vera S/N, 46022-Valencia, Spain
*Corresponding author. E-mail: jarmengo@eaf.upv.es

Summary. In the summer of 2024, table grape plants (*Vitis vinifera*, "Sweet Celebration") in Cieza (Murcia province, southeastern Spain) exhibited wood cankers and dieback symptoms consistent with Aspergillus vine canker (AVC). This study aimed to determine the aetiology of the disease and characterize the associated pathogens. Multi-locus phylogenetic analyses using *cal* and *tub* loci, combined with morphological characterization, identified *Aspergillus niger* and *A. tubingensis* from symptomatic plants. Mycelium growth patterns in response to temperature were similar for both species, with optimal growth between 30 and 33 °C, and no growth above 40 °C. Temperature also strongly influenced conidium germination. No germination occurred at 10 °C, and rapid and full germination occurred between 30 and 40 °C. Pathogenicity tests on table grape 'Alphonse Lavallée' showed that both species were pathogenic to grapevine wood, with *A. niger* exhibiting greater virulence. Inoculations on green leaves showed that both species colonized foliar tissues. These results confirm the association of *A. niger* and *A. tubingensis* with table grape cankers in southeastern Spain, and also highlight the ability of these fungi to develop at high temperatures, and pose potential threats to grape and wine production under warm Mediterranean conditions.

Keywords. *Aspergillus niger*, *A. tubingensis*, Grapevine trunk diseases, pathogenicity, *Vitis vinifera.*

OPEN ACCESS

Citation: Ali, A., León, M., Berbegal, M. & Armengol, J. (2026). Identification and characterization of *Aspergillus* species associated with Aspergillus vine canker of table grapes in Spain. *Phytopathologia Mediterranea* 65(2): 319-332. doi: 10.36253/phyto-17479

Accepted: August 30, 2026

Published: September 10, 2026

Data Availability Statement: All relevant data are within the paper and its Supporting Information files.

Competing Interests: The Author(s) declare(s) no conflict of interest.

Editor: Akif Eskalen, University of California, Davis, CA, United States.

ORCID:
AA: 0009-0008-9055-1338
ML: 0000-0003-0693-6988
MB: 0000-0002-5773-3104
JA: 0000-0003-3815-8578

INTRODUCTION

Grapevine (*Vitis vinifera* L.) is a crop of major socioeconomic importance in Spain, reinforcing this country's position as a world leader in grape production, with about 919,000 ha cultivated (OIV, 2026). However, the sustainability of Spanish viticulture is increasingly threatened by Grapevine Trunk Diseases (GTDs) caused by fungi, which pose challenges to vineyard health, longevity, and productivity (Gramaje Pérez *et al.*, 2020).

In many international table grape and wine producing regions, GTDs are among the main causes of vine decline and mortality, often leading to vine removal 10 to 15 years earlier than the expected 30 to 35 years lifespans. This premature replacement increases production costs and disrupts long-term

vineyard sustainability (Gramaje and Armengol, 2011; Mondello *et al*., 2018; Fontaine *et al*., 2025). Vineyards of all ages are susceptible to GTDs pathogens infections, which can originate as early as the nursery stage or occur later in established vineyards (Mondello *et al*., 2018).

Aspergillus vine canker (AVC), caused by *Aspergillus* spp., is a GTD affecting wine and table grapes (Fontaine *et al*., 2025). This disease has been reported in warm grape-growing regions, as *Aspergillus* spp. are favoured by hot and dry environmental conditions (Marquès *et al*., 2025). DNA-based methods have enabled inclusion of AVC within the GTD group, allowing reliable identification and classification of *Aspergillus* spp., and thus resolving previously ambiguous reports (Hong *et al*., 2005; Houbraken *et al*., 2020; Fontaine *et al*., 2025). Recent studies have shown that AVC is a distinct component within the GTD complex, rather than being a minor disease (Vitale *et al*., 2012; Bustamante *et al*., 2024, Rangel-Montoya and Hernández-Martínez, 2024; Fontaine *et al*., 2025).

AVC was first described in 1989 in the San Joaquin Valley (California, United States of America), and was later associated with reduced vine performance and canopy longevity in commercial vineyards. Follow-up studies reported that 2 to 6.1% of vines required retraining in following season, highlighting the re-establishment costs (Bustamante *et al*., 2024). In Italy, surveys conducted in southeastern Sicily (in Catania and Ragusa, between 2007 and 2009) recorded up to 18% of incidence AVC, with 2 to 4 cankers per vine persisting annually through 2010 (Vitale *et al*., 2012). In Mexico, the first national report of AVC documented up to 5% incidence, and the cultivar 'Cotton Candy' was the most susceptible, while 'Prime Seedless' was the least affected (Rangel-Montoya and Hernández-Martínez, 2024).

Infections caused by *Aspergillus* spp. on grapevines begin when conidia land on exposed or wounded tissues, particularly on fresh pruning cuts. Conidia germinate, and hyphae penetrate host plant woody tissues, typically between the cordons and the trunk of vines. Elongated, sunken cankers develop at or just below pruning or training wounds (Bustamante *et al*., 2024). Cross-sections of infected vines reveal brown to dark brown necroses spreading inward into nearby tissues, with the advancing lesions often appearing soft or spongy (Vitale *et al*., 2012; Rangel-Montoya and Hernández-Martínez, 2024). Severe lesions may girdle vascular tissues, restricting nutrient transport and leading to premature canopy decline, reduced vine vigour, and delayed budbreak (Bustamante *et al*., 2024). At the advancing margins beneath vine bark, the pathogenic fungi can produce dry black conidia, the main primary inoculum, which are dispersed in vineyards throughout growing seasons (Bustamante *et al*., 2024).

Management of AVC is due to pathogen latent infections that delay symptom detection, and the lack of effective treatments once the disease is established. Prevention of the disease using chemical, cultural, and biological measures is important (Bustamante *et al*., 2024). Pruning should avoid warm, dry conditions, and instead be performed during cool, humid periods, ensuring the removal of diseased tissues by making pruning cuts 10 to15 cm below visible symptoms. Recommended sanitation protocols include disinfecting pruning tools before, during, and after use, and protecting exposed grapevine tissues (Vitale *et al*., 2012). A key part of managing the GTD complex is protecting fresh pruning wounds with fungicides or biological control agents (e.g. *Trichoderma* spp.) immediately after pruning (Mondello *et al*., 2018; Fontaine *et al*., 2025). Trunk renewal from healthy wood can restore grape production, if applied early and followed by wound protection (Mondello *et al*., 2018).

In the summer of 2024, grapevine plants (cv. Sweet Celebration) in a table grape vineyard located in Cieza (Murcia province, southeastern Spain) exhibited cankers and dieback symptoms consistent with those described for AVC. The objectives of the present study were to determine the aetiology of the disease, and to characterize the associated pathogens.

MATERIALS AND METHODS

Sampling and fungal isolations

Four symptomatic grapevines were sampled, were cut into sections and then transported to the laboratory for fungal isolations. Wood sections (3 cm long) showing cankers were washed under running tap water, surface-sterilized using 70% ethanol, and flamed. Small internal wood chips (3–4 mm long) were then placed in Petri plates containing malt extract agar (MEA) supplemented with 0.5 g L^{-1} of streptomycin sulfate (Sigma-Aldrich) (MEAS). The plates were then incubated at 25 °C in the dark for 5 to 10 d. All emerging colonies were subcultured onto potato dextrose agar (PDA), and the subculture plates were incubated in the same conditions.

Four representative isolates (GIHF-506, GIHF-507, GIHF-508 and GIHF-509) were selected for molecular analysis, phenotypic characterization and pathogenicity tests. Single conidium isolates of each of the isolates were obtained using the serial dilution method (Dhingra and Sinclair, 2019). For long-term storage, mycelial plugs were stored at -80 °C in 1.5 mL cryovials containing 15% glycerol solution, at the fungal collection of the

Instituto Agroforestal Mediterráneo of the Universitat Politècnica de València, Spain.

Molecular identifications

Mycelium was scraped from 8-d-old PDA cultures of isolates GIHF-506, GIHF-507, GIHF-508 and GIHF-509. Total fungal DNA of each isolate was extracted using the E.Z.N.A. Plant DNA Kit (Omega Bio-tek), following the manufacturer's short protocol instructions.

Partial fragments of beta-tubulin (*tub*) and calmodulin (*cal*) genes were amplified and sequenced. Amplifications were carried out in total volumes of 20 µL using Speedy Supreme NZYTaq 2× Green Master Mix (NZYtech), according to the manufacturer's instructions, on a Peltier Thermal Cycler-200 (MJ Research). Each reaction included 10 µL of Speedy Supreme NZYTaq 2× Green Master Mix, 0.6 µL of each primer (10 µM), 1 µL of purified template DNA, and 7.8 µL of nuclease-free water. The thermal cycle consisted of an initial step of 5 min at 94 °C, followed by 35 cycles each of denaturation at 94 °C for 2 s, annealing for 5 s, and elongation at 72 °C for 5 s. A final extension was performed at 72 °C for 2 min. The primer pairs and the annealing temperatures (Ta) for each locus were as follows: BT2a and BT2b for *tub* (Ta = 55 °C) (Glass and Donaldson, 1995), and CMD5 and CMD6 for *cal* (Ta = 58 °C) (Samson *et al*., 2014). PCR products were visualized by 1.2% agarose gel electrophoresis, purified by illustra™ ExoProStar™ S (cytiva, GE Healthcare), and sequenced by the IBMCP-UPV sequencing service (Valencia, Spain). Chromatograms were checked using Sequencher software 5.0 (Gene Codes Corp.).

Sequences generated were compared with sequences in the GenBank nucleotide database, to determine the closest relatives for phylogenetic studies. For each genomic region (*tub* and *cal*), the DNA sequences obtained in the present study were aligned with reference sequences retrieved from GenBank (Table 1), using the ClustalW algorithm included in the MEGA7 soft-

Table 1. List of *Aspergillus* section *Nigri* isolates and their sequence numbers included in the phylogenetic analyses. Isolates in bold were obtained in this study from table grape samples.

Species	Isolate	Host	Country	GenBank	
				tub	*cal*
A. niger	NRRL 326 ^{T}	Tannin-gallic acid fermentation	USA	EF661089	EF661154
	CBS 101883	*Coffea robusta*	Sumatra	AY819998	EU163270
	IHEM 21604	Outdoor air	Cuba	MH614478	MH644996
	CBS 139.54	*Welwitschia mirabilis*	Namibia	FJ629291	KC480196
	IHEM 3090	Soil	Mauritius	MH614487	MH644884
	IHEM 18080	Soil of riverside	France	MH614513	MH644969
	ITAL 47.456	Surface of grape berries	Brazil	MN583579	MN583580
	GIHF-508	*Vitis vinifera*	Spain	PZ885810	PZ885814
A. brasiliensis	CBS 101740 ^{T}	Soil	Brazil	FJ629272	FN594543
	ITEM 6139	Grapes	Portugal	AM295185	AM295176
A. carbonarius	NRRL 369 ^{T}	Paper	USA	EF661099	EF661167
	NRRL 346	Unknown	Honduras	EF661098	EF661166
A. eucalypticola	DTO 53-A2 ^{T}	Soil	India	EU482435	EU482433
	NRRL 62632	*Eucalyptus* leaves	Australia	KC796360	KC796376
A. luchuensis	KACC 46772 ^{T}	Awamori-koji	Japan	JX500062	JX500071
	IHEM 25486	Human trimming liquid	France	MH614563	MH644862
A. tubingensis	NRRL 4875 ^{T}	Unknown	Unknown	EF661086	EF661151
	CBS 134.48	Unknown	Unknown	AY820007	AJ964876
	NRRL 62634	Mangrove water	Venezuela	KC796361	KC796377
	IHEM 22394	Conjunctivitis-human eye	India	MH614544	MH644870
	GIHF-506	*Vitis vinifera*	Spain	PZ885808	PZ885812
	GIHF-507	*Vitis vinifera*	Spain	PZ885809	PZ885811
	GIHF-509	*Vitis vinifera*	Spain	PZ885807	PZ885813
A. vadensis	CBS 113365 ^{T}	Dead plant tissue	Unknown	AY585531	FN594560
	IHEM 26351	Human sputum	France	MH614547	MH644878

^{T}Indicates the ex-type isolates.

ware package (Kumar *et al*. 2016). The alignments were analyzed and adjusted manually when necessary. Ambiguous sequences at either end of alignments were excluded prior to analyses. Concatenated datasets were built in Sequence Matrix v.1.8 (Vaidya *et al*., 2011).

Phylogenetic analyses were carried out using maximum parsimony (MP) and maximum likelihood (ML) approaches. Maximum parsimony analyses were carried out in MEGA X (Kumar *et al*., 2018), employing the tree Bisection and reconnection (TBR) algorithm, where gaps were treated as missing data. Topology robustness was evaluated by 1,000 bootstrap replications (Felsenstein, 1985). Measures for maximum parsimony, as tree length (TL), consistency index (CI), and retention index (RI), were also calculated. Maximum likelihood analyses were carried out using IQ-TREE v.3.1.2 (Wong *et al*., 2026). The concatenated dataset was partitioned into the *tub* and *cal* genomic regions, and the best-fit evolutionary models were selected using ModelFinder (Kalyaanamoorthy *et al*., 2017), based on the Bayesian information criterion (BIC). HKY+I was selected for *tub*, and HKY+G4 for *cal*. Branch support was assessed using 1,000 ultrafast bootstrap (UFBoot) replicates, and 1,000 SH-like approximate likelihood ratio test (SH-aLRT) replicates.

Morphological characterizations

Isolates GIHF-506 and GIHF-508 were used for morphological characterizations. Petri plates containing PDA or Czapek agar (CZA; 30.0 g L^{-1} sucrose, 2.0 g L^{-1} $NaNO_3$, 0.5 g L^{-1} KCl, 0.5 g L^{-1} Mg-glycerophosphate, 0.35 g L^{-1} K_2SO_4, 0.01 g L^{-1} $FeSO_4$, 12.0 g L^{-1} agar) were inoculated with 5 mm mycelium plugs taken from actively growing margins of a 7-d-old cultures. After 7 d of incubation at 25 °C in darkness, colony morphologies were recorded, including; obverse and reverse colours, texture (e.g., velvety *vs*. granular/fluffy), and margin appearance (smooth to slightly lobed). Microscopic features were assessed from 4- to 7-d old cultures. Mycelium and black conidia were mounted in Shear's fluid (50 mL of 2% potassium acetate, 20 mL glycerol, 30 mL of 95% ethanol), and examined at 10 ×, 20 ×and 40 × magnifications, using a Nikon Eclipse Ni microscope equipped with NIS-Elements-D imaging software. Vesicle and conidium diameters were measured for 50 replicates per structure and per isolate.

Mycelium growth at different temperatures

Isolates GIHF-506, GIHF-507, GIHF-508 and GIHF-509 were grown on PDA in 90 mm diam. Petri plates (~20 mL per plate). For each assay plate, a 5 mm diam mycelium plug was taken from the active margin of a 7-d-old culture, and placed (mycelium side down) in the centre of a fresh PDA plate. Growth was evaluated at 10, 15, 20, 25, 30, 35, 40, or 45 °C. For each isolate-temperature combination, four replicates were prepared. The experiment was repeated (two independent runs), resulting in a total of eight replicates per isolate–temperature combination. Inoculated plates were sealed with parafilm, randomized inside incubators, and kept for 7 to 21 d (depending on the temperature) in the dark. When the diameter (D, mm) of a colony on the medium reached 60-70% of the Petri dish diameter, it was measured along two perpendicular axes and averaged once uniform growth was established. The time elapsed from inoculation to measurement (t, d) was recorded. The average radial growth rate was calculated as:

$$\text{Growth rate (mm d}^{-1}) = [(D - 5\text{ mm}) / 2] / t;$$

where (D – 5 mm) / 2 was the radial increase from each inoculum plug edge to the colony edge. If no growth was observed by the endpoint, the rate was recorded as 0 mm d^{-1}.

The data obtained were rescaled to 0 to 1, by dividing each datum by the maximum datum obtained in each experiment. Rescaled data were regressed against temperature, and nonlinear regression equations were compared based on data representation. A beta equation was fitted to the data in the following form (Analytis, 1977):

$$y = [a \times \text{Teq}^b \times (1 - \text{Teq})]^c;$$

where: y = rescaled daily growth (0 to 1); Teq = temperature equivalent calculated as Teq = (T − T min) / (T max– T min): where T = temperature (°C); T min and T max = minimum and maximum temperatures for mycelium growth; and *a* to *c* = the equations parameters. T min for mycelium growth was 9 °C and T max was 44 °C, (Gougouli and Koutsoumanis, 2010). All data analyses were performed using R version 4.6.1 via RStudio version 2026.07.1 (Posit Team, 2026).

Equation parameters were estimated using the function *nls* included in the package "stats" (Wickman, 2019). Goodness-of-fit of the equations was evaluated based on the adjusted R^2, the concordance correlation coefficient (CCC), and the root mean square error (RMSE) (Lin, 1989). Linear regressions were carried out between the observed and the predicted data, to estimate the adjusted R^2, using the *lm* function of the R "stats" package. The CCCs were obtained using the *epi.ccc* function of the R

"epiR" package (Carstensen *et al*., 2022). The RMSEs, were obtained using the *rmse* function of the R "modelr" package (Wickham, 2019). According to Analytis (1977), the optimum temperatures (T opt) for daily mycelium growth were calculated as follows:

$$T\ opt = [(b \times c) / (b \times c + c)] \times (T\ max - T\ min) + T\ min;$$

where b and c are equation parameters, and T max and T min are as described above.

Conidium germination at different temperatures and time periods

Isolates GIHF-506 and GIHF-508 were used for this study. Conidium suspensions were obtained from 7-d-old PDA cultures by gently flooding respective colonies with sterile water containing a non-ionic surfactant (~ 0.01% Tween), loosening the conidia with a sterile loop, and filtering the resulting conidium suspensions through sterile gauze to remove hyphal fragments. Conidium concentrations were adjusted to 10^5 conidia mL^{-1} using hemocytometer counts. For each isolate-temperature-time combination, two 20 µL drops of conidium suspension were deposited onto the surface of a fresh 90 mm diam PDA plate, and the plates were incubated in the dark at the respective specified temperatures. Conidium germination was assessed at 6, 12, 18, 24, 36, and 48 h after plating. The experiment was repeated (two independent runs, with four replicates per run). At the end of each incubation period, conidium germination was determined by examining 100 conidia per drop using a microscope (× 40 magnification). A conidium was considered germinated when the length of the germtube exceeded the length of the conidium. Mean germination percentages were then calculated for each treatment, and statistical analyses were not carried out because this experiment was intended to be descriptive.

Pathogenicity test on table grape plants

For pathogenicity tests, rooted cuttings of table grape 'Alphonse Lavallée' were transplanted into 3 to 5 L capacity pots that were maintained in a greenhouse until inoculation, allowing a single shoot to develop on each cutting. Isolates GIHF-506 and GIHF-508 were tested using four plants per isolate, with an equal number of non-inoculated plants as inoculation controls. Inoculum consisted of 6 mm mycelium plugs taken from the advancing margins of 3 to 7-d-old PDA cultures. On each plant, a 6 mm diam. circular wound was made to the cambium at an internode of the main shoot, using a sterile cork borer. A mycelium plug was inserted (mycelium facing the cambium), was then covered with moist cotton, and then sealed with Parafilm to prevent desiccation. Plants were then arranged randomly in a greenhouse under semi controlled conditions (~35 °C day / 25 °C night), were irrigated as needed, and then inspected weekly for external symptoms. The experiment was performed twice (n = 8 plants per isolate in total).

The necrotic lesion length (mm) developed on each shoot was measured 50 d after inoculation, and mean lesion lengths were calculated. Small wood chips from lesion margins were surface-disinfected, and then plated on MEAS to assess completion of Koch's postulates. All emerging colonies were transferred to PDA plates and incubated at 25 °C in darkness until sporulation. The effect of the inoculated isolate, the experiment and the interaction on lesion length was analyzed using a generalized linear model (GLM) with a Gamma distribution and a log link function. The dispersion and residuals of the models were tested by using the function *simulateResiduals* of the "DHARMa" package. Once significance of factors was assessed pairwise comparisons of adjusted means were performed using the "emmeans" package (Lenth and Piaskowski, 2026) with Bonferroni correction adjustment and grouping letters were generated using the *cld* function with "multcomp" package (Hothorn *et al*., 2008).

Pathogenicity on leaves

The pathogenicity of isolates GIHF-506 and GIHF-508 was evaluated on detached leaves of table grape cv. 'Alphonse Lavallée' following the methods described by Rangel-Montoya and Hernández-Martínez (2024). Mature, healthy leaves without visible symptoms, wounds, or insect injury were collected, then gently rinsed with sterile water, and air-dried. For each isolate, eight leaves were inoculated, while an additional eight leaves served as non-inoculated controls.

Conidium suspensions were prepared from 3-d-old PDA cultures, and were adjusted to 10^5 conidia mL^{-1} in sterile water using a hemocytometer. For inoculation, each leaf was positioned abaxial side up. The petiole-lamina junction was punctured once with a sterile entomological needle, and a 10 µL droplet of conidium suspension was applied to the wound, to facilitate capillary entry and ensure uniform inoculation. Non-inoculated control leaves received 10 µL droplets of sterile water following the same procedure.

Inoculated and non-inoculated control leaves (four per isolate) were placed in humid chambers (sealed plas-

tic boxes containing moistened sterile filter paper) to maintain high relative humidity (>95%). These were kept for 10 d in an incubator at 25 °C with a 12 h light, 12 h darkness daily cycle. The filter paper was re-moistened periodically to maintain humidity, ensuring no direct water contact with the leaf surfaces. The experiment was performed twice.

Disease severity was visually assessed at the end of the incubation period, using a 0–5 scale (Montoya and Hernández-Martínez, 2024), where: 0 = no symptoms; 1 = slight wilting; 2 = red necrotic lesions; 3 = mycelium growth; 4 = conidium presence; 5 = mycelial growth and conidium presence. Severity data was transformed using the McKinney Index (MKI), a widely applied disease severity index for ordinal data (McKinney, 1923; Bock *et al*., 2024). The effect of the inoculated isolate and the experiment on disease severity were analyzed using Kruskal–Wallis rank-sum test by *kruskal_test* function of the "rstatix" package (Kassambara, 2026). Once significance of effects was assessed, pairwise comparisons were performed using Dunn's test with Bonferroni adjustment.

RESULTS

Sampling and fungus isolations

Symptoms observed in the table grape orchard are shown in Figure 1 A. Affected plants exhibited wilting and decay, along with cankers on the main trunks, and internal wood necroses (Figure 1, B and C). Isolations from symptomatic tissues consistently recovered *Aspergillus* colonies, characterized by rapid radial growth and profuse dark sporulation (Figure 1 D). From these primary cultures, the four representative isolates (GIHF-506, GIHF-507, GIHF-508, GIHF-509) were selected.

Molecular identifications

PCR amplification of the β-tubulin (*tub*) and calmodulin (*cal*) gene regions yielded single, well-defined amplicons of, respectively, approx. 550 bp and 600 bp, for all four fungal isolates. Purified PCR products were sequenced, and chromatograms were manually inspected. BLASTn analyses of the obtained sequences against the NCBI GenBank database showed ≥99% similarities with *A. tubingensis* and *A. niger*.

Multi-locus phylogenetic analyses of concatenated *tub* and *cal* alignments were conducted using the Maximum Parsimony (MP) method in MEGA X and the Maximum Likelihood (ML) method in IQ-TREE v.3.1.2

Figure 1. Field symptoms associated with *Aspergillus* infections in grapevines. (A) Decline symptoms in a vineyard. (B) External discolouration and tissue damage on a trunk. (C) Trunk cross sections showing internal necroses. (D) Colonies of *Aspergillus* isolated from infected grapevine tissues.

(Figure 2). The analyses included 25 taxa: 19 reference taxa representing the six species within section Nigri of *Aspergillus*, the four isolates analyzed in this study, and two *A. carbonarius* isolates used as the outgroup. The combined dataset comprised 975 positions including gaps (488 from *tub* and 487 from *cal*), of which 258 (26.5%) were parsimony-informative. MP analyses yielded nine most-parsimonious trees (TL = 372, CI = 0.89, RI = 0.99); one of which is shown in Figure 2. The resulting phylogeny resolved the six species into the three main phylogenetic lineages of section Nigri. Three of the isolates from the present study (GIHF506, GIHF507, and GIHF509) clustered unambiguously within the *A. tubingensis* species clade, which forms part of the *A. tubingensis* lineage, and isolate GIHF508 clustered within the *A. niger* species clade. The ML analysis produced a topology highly congruent with the MP analysis, confirming the same three major phylogenetic lineages and placement of the four isolates within the *A. tubingensis* and *A. niger* species clades (Figure 2).

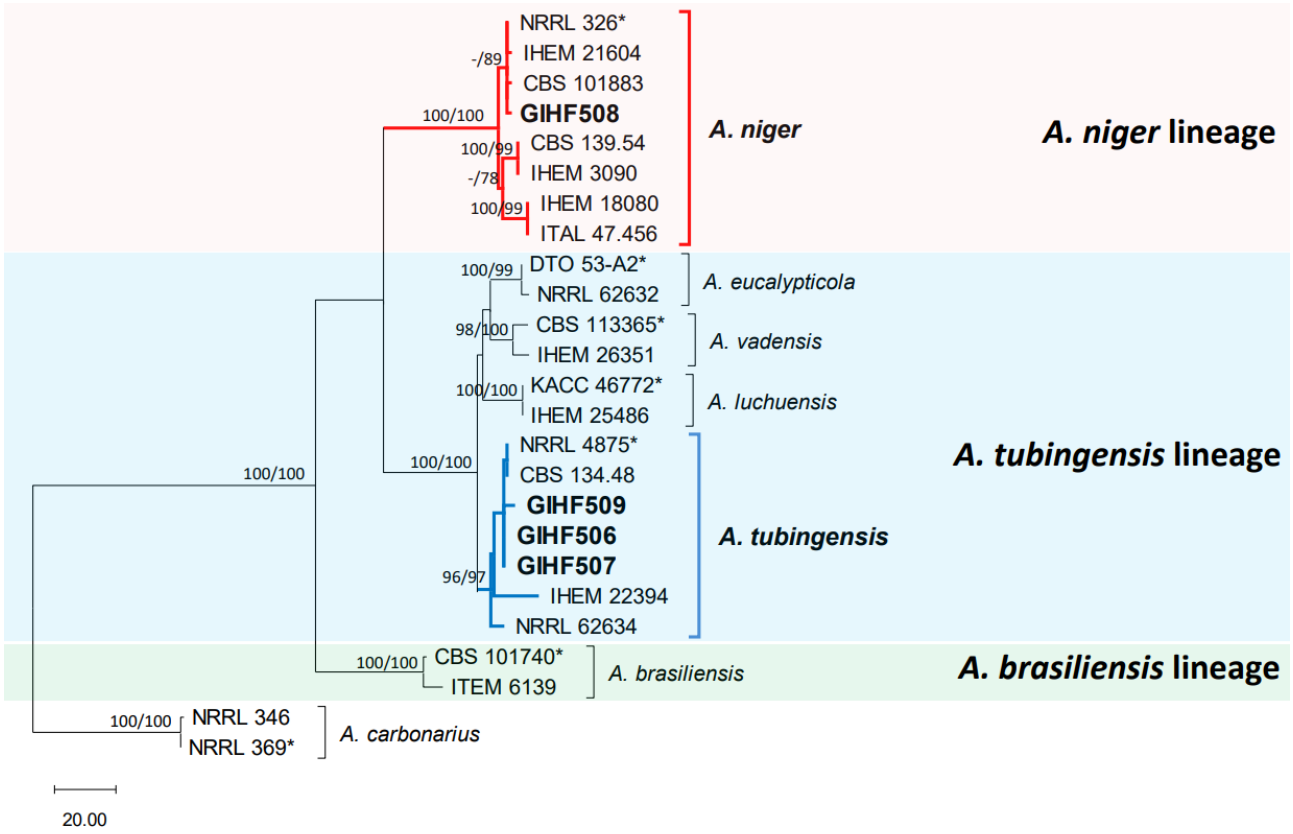

Figure 2. One of nine most parsimonious trees obtained from the analysis of the combined sequence data of two loci (beta-tubulin and calmodulin) of 25 *Aspergillus* isolates. Scale bar shows 20 changes, and bootstrap support values from 1,000 replicates for Maximum Likelihood (ML) and Maximum Parsimony (MP) analyses are indicated at the tree nodes (ML/MP). Values below 95% for ML and 70% for MP are not shown. The ex-type isolates are labelled with an asterisk, and the *Aspergillus* spp. isolated in the present study are highlighted in bold font. The tree was rooted to *A. carbonarius* (NRRL 369 and NRRL 346).

Morphological characterizations

After 4 to 7 d incubation at 25 °C in darkness, distinct colony characteristics were observed on CZA and PDA media for the representative isolates of *A. niger* (GIHF-508) and *A. tubingensis* (GIHF-506). On CZA, *A. niger* maintained dense black sporulation, with reverse pigmentation ranging from colourless to pale yellow. In contrast, *A. tubingensis* showed more variable sporulation intensity, and had yellowish reverse pigmentation. On PDA, the *A. niger* isolate developed colonies with intense black sporulation, granular texture, and well-defined white margins, while *A. tubingensis* had olive-green to black sporulation, with floccose aerial mycelium and well-defined white margins. Microscope examination revealed that both *A. niger* and *A. tubingensis* produced globose to subglobose conidia and spherical vesicles, typical of section Nigri, and had typical biseriate conidium structures. *Aspergillus niger* displayed robust conidiophores with prominent vesicles, dense conidium chains, and black, strongly echinulate, conidia. *Aspergillus tubingensis* developed less robust conidiophores, less compact conidium chains, and brown finely roughened conidia. Both fungi produced globose conidium heads. Conidium diameters of *A. niger* ranged from 3.05 to 4.75 µm (mean = 3.90 ± 0.42 µm), while those of *A. tubingensis* ranged from 2.85 to 4.65 µm (mean = 3.74 ± 0.38 µm). Vesicle diameters for *A. niger* varied from 36.39 to 73.39 µm (mean = 54.06 ± 8.37 µm), and from 41.30 to 61.17 µm (mean = 51.48 ± 6.12 µm) for *A. tubingensis*.

Mycelium growth at different temperatures

Curves that fit the temperature response to daily mycelium growth rates are shown in Figure 3. Equation parameters with their standard errors and goodness-of-fit coefficients are summarized in Table 2. In general, mycelium growth occurred between 15 and 40 °C, with radial expansion increasing with temperature, from 15 °C up

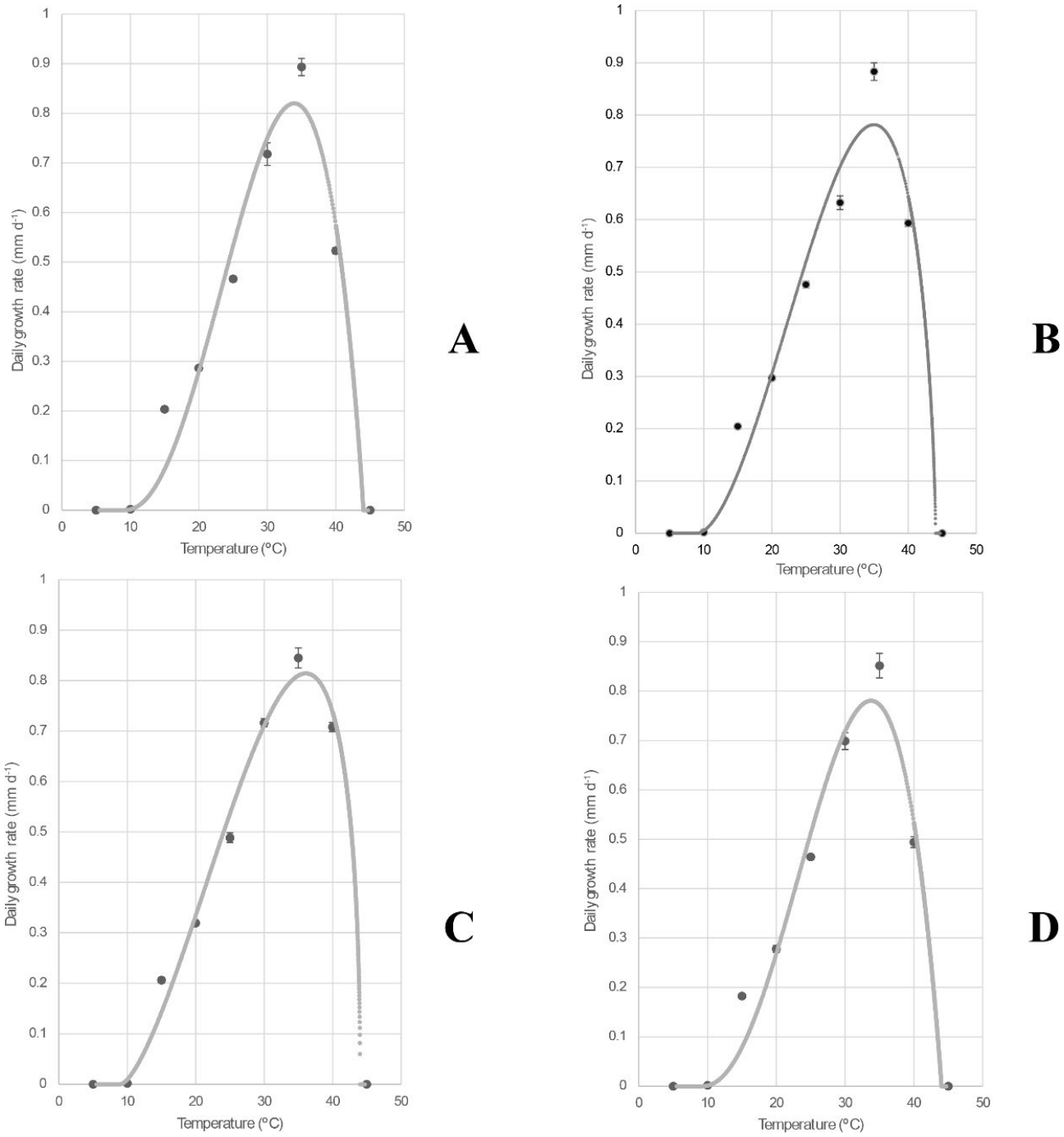

Figure 3. Mean mycelium growth rates of *Aspergillus* isolates at different temperatures. (A) Isolate GIHF-506, (B) GIHF-507, (C) GIHF-508, and (D) GIHF-509. Observed mean daily growth rates (points) are shown together with the fitted temperature response model (gray lines).

to a peak between 30 °C and 35 °C, followed by a sharp decline. At 15 °C, colony development was very slow (≤ 1 mm day^{-1}), and increased with increasing temperature, reaching mean radial rates of approx. 1.5 to 3.5 mm d^{-1} at 20–25 °C, while the greatest rates (6 to 8 mm d^{-1}) were recorded at 30 to 35 °C. At 40 °C, growth was substantially reduced (≤ 1 mm d^{-1}) and no mycelium growth occurred at 45 °C. Calculated optimum temperatures for growth ranged from 30.2 °C to 33.4 °C. The lower optimum temperature was recorded for *A. niger* isolate GIHF-

Table 2. Parameters and goodness-of-fit coefficients for equations used to describe the effect of temperature on daily mycelial growth of *Aspergillus niger* (GIHF-508) and *A. tubingensis* (GIHF-506, GIHF-507 and GIHF-509) isolates.

Isolate	Topt[a]	Estimated parameters ± SE			Goodness-of-fit		
		a	b	c	Adjusted R^{2b}	CCC[c]	RMSE[d]
GIHF-506	33.4	5.70 ± 3.14	2.30 ± 0.53	0.93 ± 0.27	0.9456	0.9759	0.0631
GIHF-507	31.2	3.15 ± 1.56	1.82 ± 0.47	0.63 ± 0.24	0.9404	0.9744	0.0623
GIHF-508	30.2	2.36 ± 0.61	1.54 ± 0.24	0.45 ± 0.12	0.9823	0.9925	0.0349
GIHF-509	33.4	5.67 ± 2.84	2.32 ± 0.48	0.96 ± 0.25	0.9535	0.9795	0.0559

[a]: Predicted optimal temperature (Analytis, 1977); [b]: adjusted coefficient of determination; [c]: concordance correlation coefficient; [d]: root mean square error.

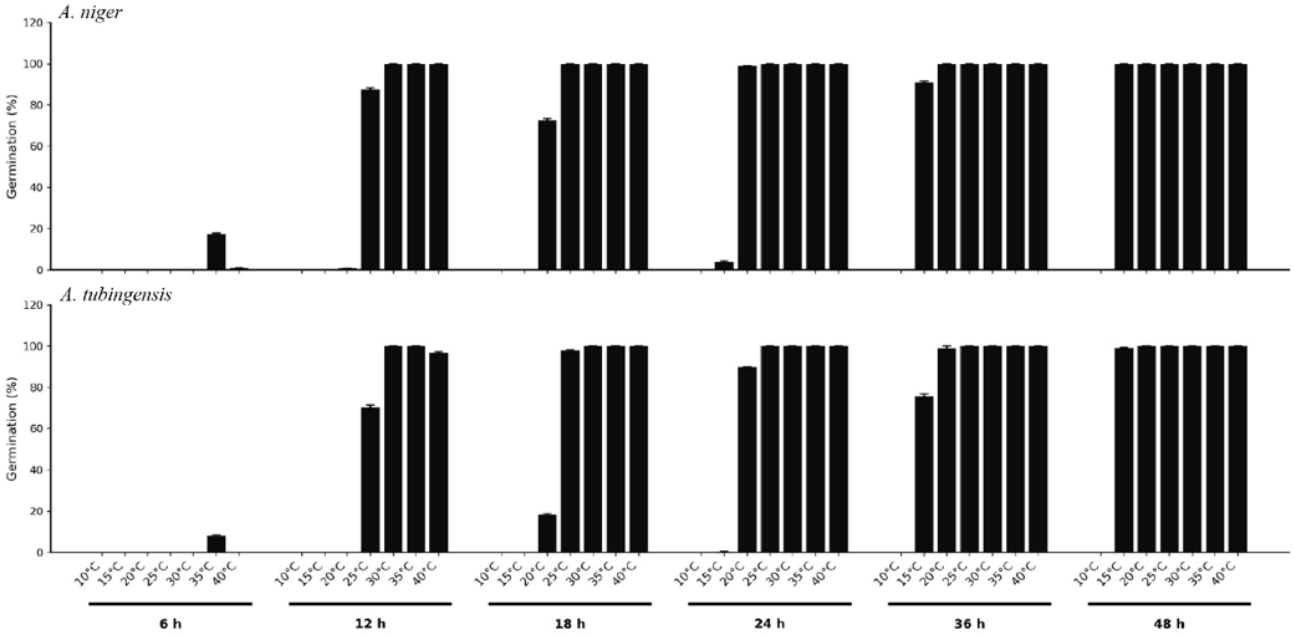

Figure 4. Mean conidium germination (%) of *Aspergillus niger* (upper histogram) and *A. tubingensis* (lower) at different temperatures (10 to 40 °C) over time intervals of 6, 12, 18, 24, 36, or 48 h). Bars accompanying each symbol represent standard error.

508 (Table 2). In general, the growth response equations provided a good fit of data, with adjusted R^2 values ranging from 0.9404 to 0.9823, and RMSE ranging from 0.0349 to 0.0631 (Table 2). CCC values were 0.99 for the equation describing the growth of the *A. niger* isolate, and 0.97 for the equations of *A. tubingensis* isolates.

Conidium germination at different temperatures and time periods

Conidium germination was influenced by temperature and incubation time, with *A. niger* generally initiating germ tube emergence slightly earlier than *A. tubingensis* (Figure 4). No germination occurred at 10 °C even after 48 h of incubation, indicating that this temperature was below the physiological threshold for germination. Consequently, responses are described for 15 to 40 °C.

After 6 h, no germination was observed between 15 °C and 30 °C for either species. At 35 °C, *A. niger* reached 17% germination, and *A. tubingensis* reached 8% germination, while only 1% germination was recorded for *A. niger* at 40 °C. After 12 h, conidia remained dormant at 15 °C. At 20 °C, *A. niger* showed 1% germination, whereas at 25 °C germination rates were greater (86% in *A. niger*; 73% in *A. tubingensis*). Complete germination (100%) was achieved at 30 to 35 °C for both species, and nearly so (96%) at 40 °C. After 18 h, while no germination occurred at 15 °C, *A. niger* reached 75%, and *A. tubingensis* 21%, at 20 °C. Both isolates attained 100%

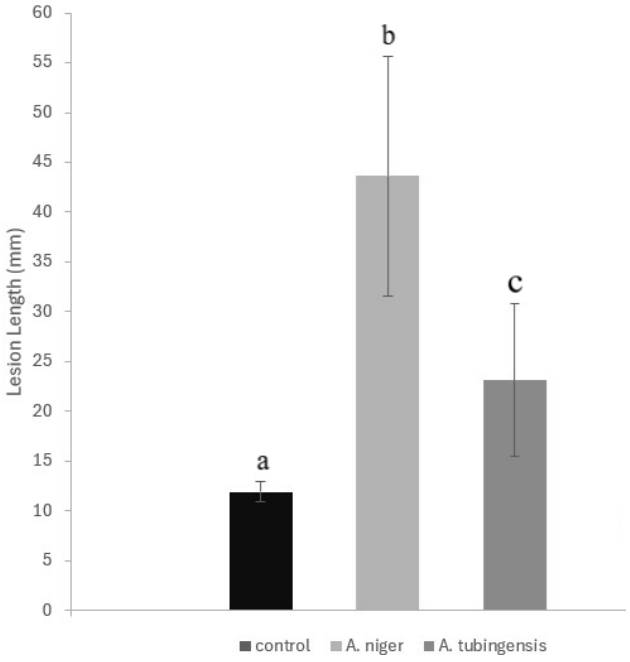

Figure 5. Mean lesion lengths in grapevine stems caused by *Aspergillus niger* and *A. tubingensis* isolates, compared with non-inoculated controls. Bars accompanying each mean represent standard errors, and different letters indicate statistically significant differences between the means, as shown by Bonferroni-adjusted pairwise comparisons of the means.

conidium germination between 25 and 40 °C. After 24 h germination was initiated at 15 °C (3% in *A. niger*, 1% in *A. tubingensis*), while at 20 °C, *A. niger* reached 100%, and *A. tubingensis* 90%. After 36 h, germination at 15 °C reached of 92% for *A. niger* and 79% for *A. tubingensis*. After 48 h, complete germination (100%) was achieved at all temperatures from 15 to 40 °C.

Pathogenicity test on grapevine plants

After 50 d incubation, both *A. niger* and *A. tubingensis* induced characteristic AVC symptoms on the inoculated grapevine shoots, while non-inoculated control plants remained symptomless. Necrotic lesions developed around the inoculation sites and extended longitudinally along the internodes. Darkened vascular tissues and black conidium masses were evident beneath the bark of inoculated plants.

The inoculated fungi were successfully re-isolated from all symptomatic tissues (100% re-isolation frequency), thereby fulfilling Koch's postulates. Mean lesion lengths differed significantly among the inoculated isolates (Figure 5), with the longest lesions produced by *A. niger* (43.62 ± 12.01 mm), followed by *A. tubingensis* (23.12 ± 7.65 mm). The non-inoculated control plants had limited discolourations around the wound sites (11.87 ± 1.02 mm).

Statistical analyses of lesion length data showed statistically significant effects on lesion development. However, no significant effect was observed for the experiment or the experiment × isolate interaction, indicating consistent symptom development across the two experimental repetitions. *Post hoc* comparisons showed significant differences among the isolates (Figure 5). and both inoculated isolates of *Aspergillus* spp. produced larger lesions than for the non-inoculated controls.

Pathogenicity test on grapevine leaves

Pathogenicity tests conducted on detached leaves of cv. 'Alphonse Lavallée' revealed significant differences in disease severity among inoculated isolates after 10 d of incubation (Figures 6 and 7). While most non-inoculated control leaves had no visible symptoms, one leaf exhibited slight wilting (severity = 1), resulting in a mean severity index of 0.12. In contrast, inoculated leaves developed characteristic red necrotic lesions and sporulation at the infection sites, consistent with *Aspergillus* infections.

Leaves inoculated with *A. niger* exhibited variable responses, with symptom severity ranging from 0 to 5 (mean severity index = 2.63), Red-necrotic lesions and localized mycelium growth were frequently observed, and some leaves developed black conidium masses at the inoculation sites. *Aspergillus tubingensis* induced the most severe symptoms, with seven out of the eight inoculated leaves reaching the maximum severity score (5), characterized by extensive mycelium growth and abundant conidium formation. The mean severity index for *A. tubingensis* was 4.38.

Statistical analyses confirmed a significant effect ($P < 0.001$) of the inoculations on leaf symptom severity relative to the non-inoculated controls. However, no effect ($P = 0.596$) was observed for the experiment. *Post hoc* comparisons indicated that while both *Aspergillus* species caused greater disease severity than the non-inoculated controls, the differences between the two fungal species were not statistically significant (Figure 7).

DISCUSSION

This study provides the first report of Aspergillus vine canker (AVC) affecting table grapevine in Spain. Etiology of this disease was established through morphological and molecular pathogen characterization, *in*

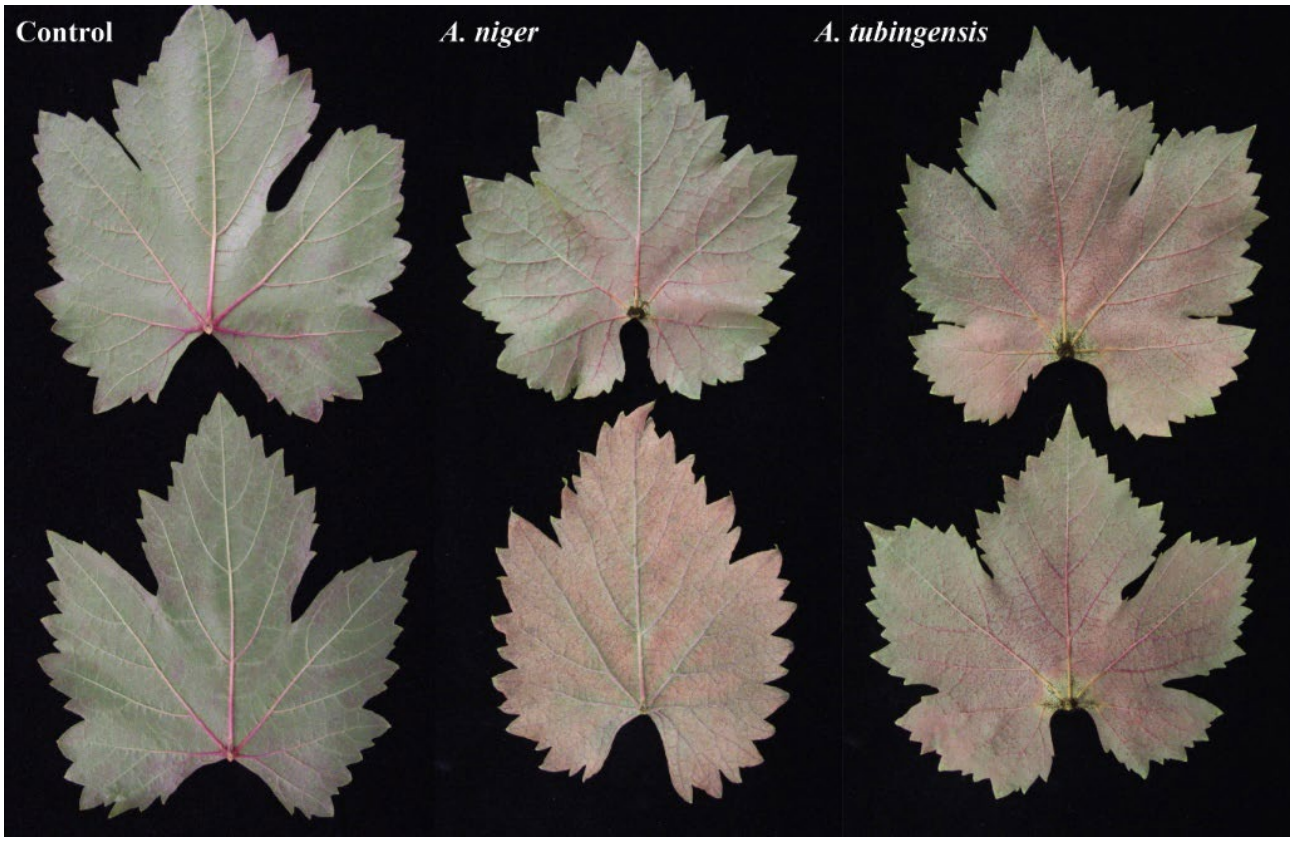

Figure 6. Grapevine leaf symptoms caused by *Aspergillus niger* or *A. tubingensis*, compared with symptomless non-inoculated control leaves (left).

vitro assays assessing mycelium growth and conidium germination of *Aspergillus* isolates under varying temperatures, and their pathogenicity to grapevine plants and leaves.

These results identified *A. niger* and *A. tubingensis* associated with AVC symptomatic plants. The combined use of *cal* and *tub* loci were effective for precise species level identifications within *Aspergillus* section Nigri, enabling differentiation of closely related taxa (Vitale *et al*., 2012). Morphological analyses also provided differentiation between these two species, confirming the results of the molecular identification. *Aspergillus tubingensis* was the predominant species, accounting for most isolates recovered from symptomatic table grape cankers, while *A. niger* occurred less frequently, indicating its coexistence with *A. tubingensis* in the AVC complex.

These results are consistent with those from other grape-producing regions. In Sicily, *A. tubingensis* and *A. niger* were identified as the main species associated with AVC, both capable of inducing lesions on woody grapevine tissues (Vitale *et al*., 2012). Bustamante *et al*., (2024) also reported *A. tubingensis* as the dominant species responsible for AVC and summer bunch rot in California, whereas *A. niger* was detected at lower frequency. Similar results were observed in Mexico, where *A. tubingensis* and *A. niger* were confirmed as the causal agents of AVC in several table grape cultivars (Rangel-Montoya and Hernández-Martínez, 2024).

Regarding effects of temperature on mycelium growth, both species showed similar patterns, but *A. niger* consistently had slightly faster radial growth than the *A. tubingensis* isolates across most temperatures assessed. The optimal growth temperatures were between 30 and 33 °C, and no growth occurred above 40 °C, which aligns with previously described thermal profiles for *Aspergillus* species involved in AVC (Vitale *et al*., 2012; Bustamante *et al*., 2024; Rangel-Montoya and Hernández-Martínez, 2024). Temperature also strongly influenced conidium germination of both species. The absence of germination at 10 °C showed that this temperature was below the physiological threshold, while the rapid and complete germination between 30 and 35 °C identified the optimum range, corresponding to observations of temperature effects on mycelium growth.

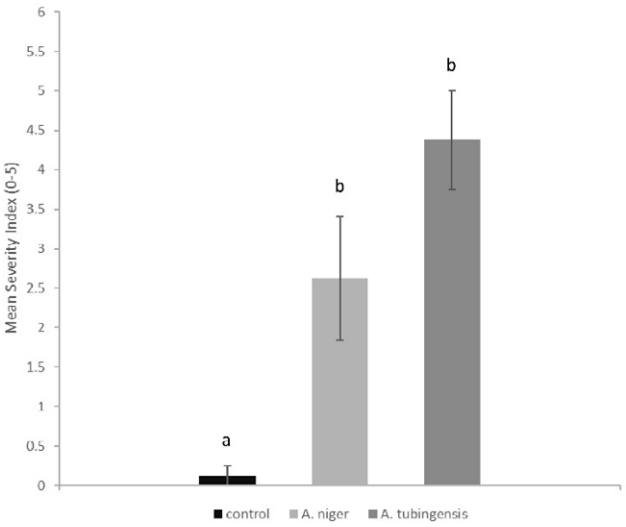

Figure 7. Mean severity indices for grapevine leaves inoculated with *Aspergillus* isolates. Mean severity index (0 to 5 scale) was recorded for leaves following plant inoculations with *A. niger* or *A. tubingensis*, compared with the non-inoculated controls. Bars represent mean severty index ± standard errors. Different letters indicate differences ($P \leq 0.05$), according to Bonferroni-adjusted pairwise comparisons of means.

The ability of conidia to germinate at 40 °C demonstrated high thermal tolerance in the isolates assessed.

These results indicate that *A. niger* and *A tubingensis* are both adapted to periods of elevated environmental temperatures typical of Mediterranean and semi-arid summers (Houbraken *et al*., 2020; Rangel-Montoya and Hernández-Martínez, 2024), and are consistent with previous findings. In Italy and California, *A. niger* and *A. tubingensis* were confirmed as the main agents of AVC, and were shown to thrive in warm, semi-arid vineyards (Vitale *et al*., 2012; Bustamante *et al*., 2024). Mexican isolates (*A. tubingensis*, *A. niger* and *A. welwitschiae*) survived temperatures of up to 40 to 50 °C (Rangel-Montoya and Hernández-Martínez, 2024). Seasonal aerobiology studies carried out by Bustamante *et al.* (2024) revealed sustained, warm season conidium production. Traps placed in table grape vineyards in Kern County, California, from late spring through summer, repeatedly captured *Aspergillus*, indicating that airborne inoculum can persist for weeks to months rather than appearing in brief pulses.

The pathogenicity tests performed on table grape plants cv. 'Alphonse Lavallée' demonstrated that both *A. niger* and *A. tubingensis* are pathogenic to grapevine wood, with *A. niger* exhibiting greater virulence than *A. tubingensis*, which is consistent with reports from Italy (Vitale *et al*., 2012), California (Bustamante *et al*., 2024), and Mexico (Rangel-Montoya and Hernández-Martínez, 2024). Grapevine leaf inoculations with *A. niger* and *A. tubingensis* also showed that both species can colonize grapevine leaf tissues. Development of necroses, mycelium growth, and black conidial masses on inoculated leaves, corroborates results of foliar inoculations reported in previous studies in Mexico (Rangel-Montoya and Hernández-Martínez, 2024), confirming the ability of these species to infect woody and green grapevine tissues.

Overall, the present study results confirm that *A. niger* and *A. tubingensis* are associated with table grape cankers in southeastern Spain, and highlight the ability of these fungi to develop under high temperatures, posing potential threats to grape and wine production under warm Mediterranean climatic conditions.

ACKNOWLEDGMENTS

This research was funded by the European Union. Views and opinions expressed are however those of the author(s) only and do not necessarily reflect those of the European Union or the European Education and Culture Executive Agency (EACEA). Neither the European Union nor EACEA can be held responsible for them.

LITERATURE CITED

Analytis S., 1977. On the relation between biological development and temperature of some plant pathogenic fungi. *Journal of Phytopathology* 90: 64–76. https://doi.org/10.1111/j.1439-0434.1977.tb02886.x

Bock C.H., Del Ponte E.M., Chiang K.-S., 2024. The nuances of plant disease severity estimation using quantitative ordinal scales—Lessons learned over four decades. *Phytopathology* 114(6): 1157–1159. https://doi.org/10.1094/phyto-11-23-0435-le

Bustamante M.I., Elfar K., Kuzmenko J., Zaninovich T., Arreguin M., ... Eskalen A., 2024. Reassessing the etiology of Aspergillus vine canker and summer bunch rot of table grapes in California. *Plant Disease* 108(4): 941–950. https://doi.org/10.1094/PDIS-06-23-1137-RE

Carstensen B., Plummer M., Laara E., Hills M., 2022. Epi: A Package for Statistical Analysis in Epidemiology. https://CRAN.R-project.org/package=Epi

Dhingra O.D., Sinclair J.B., 2019. Basic Plant Pathology Methods. 2nd edition. CRC Press, Boca Raton, Florida, USA. https://doi.org/10.1201/9781315138138

Felsenstein J., 1985. Confidence limits on phylogenies: An approach using the bootstrap. Evolution 39:

783–791. https://doi.org/10.1111/j.1558-5646.1985.tb00420.x

Fontaine F., Trouillas F.P., Armengol J., Eskalen A., 2025. Fungal trunk diseases: A global threat to grapevines. *Annual Review of Phytopathology* 63: 577–602. https://doi.org/10.1146/annurev-phyto-121323-022259

Glass N.L., Donaldson G.C., 1995. Development of primer sets designed for use with the PCR to amplify conserved genes from filamentous ascomycetes. *Applied and Environmental Microbiology* 61(4): 1323–1330. https://doi.org/10.1128/AEM.61.4.1323-1330.1995

Gougouli M., Koutsoumanis K.P., 2010. Modelling growth of *Penicillium expansum* and *Aspergillus niger* at constant and fluctuating temperature conditions. *International Journal of Food Microbiology* 140(2–3): 254–262. https://doi.org/10.1016/j.ijfoodmicro.2010.03.021

Gramaje D., Armengol J., 2011. Fungal trunk pathogens in the grapevine propagation process: Potential inoculum sources, detection, identification, and management strategies. *Plant Disease* 95(9): 1040–1055. https://doi.org/10.1094/PDIS-01-11-0025

Gramaje Pérez D., Armengol Fortí J., Barajas Tola E., Berbegal Martínez M., Chacón Vozmediano J.L., … Sagüés Sarasa A., 2020. Guía sobre las enfermedades fúngicas de la madera de la vid. Ministerio de Agricultura, Pesca y Alimentación (MAPA), Madrid, Spain.

Hong S.-B., Go S.-J., Shin H.-D., Frisvad J.C., Samson R.A., 2005. Polyphasic taxonomy of *Aspergillus fumigatus* and related species. *Mycologia* 97(6): 1316–1329. https://doi.org/10.1080/15572536.2006.11832738

Hothorn T., Bretz F., Westfall P., 2008. Simultaneous Inference in General Parametric Models. *Biometrical Journal* 50: 346–363. https://doi.org/10.1002/bimj.200810425

Houbraken J., Kocsubé S., Visagie C.M., Yilmaz N., Wang X.-C., … Frisvad J.C., 2020. Classification of *Aspergillus*, *Penicillium*, *Talaromyces* and related genera (Eurotiales): An overview of families, genera, subgenera, sections, series and species. *Studies in Mycology* 95: 5–169. https://doi.org/10.1016/j.simyco.2020.05.002

Kalyaanamoorthy S., Minh B.Q., Wong T.K., Von Haeseler A., Jermiin L. S., 2017. ModelFinder: fast model selection for accurate phylogenetic estimates. *Nature methods*, 14: 587–589. https://doi.org/10.1038/nmeth.4285

Kassambara, A. Rstatix: Pipe-Friendly Framework for Basic Statistical Tests Available online: https://cran.r-project.org/web/packages/rstatix/index.html (accessed on 31 August 2026).

Kumar S., Stecher G., Tamura K., 2016. MEGA7: Molecular evolutionary genetics analysis version 7.0 for bigger datasets. *Molecular Biology and Evolution* 33(7): 1870–1874. https://doi.org/10.1093/molbev/msw054

Kumar S., Stecher G., Li M., Knyaz C., Tamura K., 2018. MEGA X: Molecular evolutionary genetics analysis across computing platforms. Molecular *Biology and Evolution* 35: 1547–1549. https://doi.org/10.1093/molbev/msy096

Lenth R., Piaskowski J., 2026. emmeans: Estimated Marginal Means, aka Least-Squares Means. https://rvlenth.github.io/emmeans/

Lin L.I., 1989. A concordance correlation coefficient to evaluate reproducibility. *Biometrics* 45:255-268.

Marquès J., Castellà G., Bragulat M.R., Cabañes F.J., 2025. Diversity of *Aspergillus* section Nigri species from vineyards with different agro-climatic conditions in Catalonia, Spain. International *Journal of Food Microbiology* 430: 111049. https://doi.org/10.1016/j.ijfoodmicro.2024.111049

McKinney H.H., 1923. Influence of soil temperature and moisture on infection of wheat seedlings by *Helminthosporium sativum*. *Journal of Agricultural Research* 26: 195–217. https://doi.org/10.5555/19241100488

Mondello V., Songy A., Battiston E., Pinto C., Coppin C., … Fontaine F., 2018. Grapevine trunk diseases: A review of fifteen years of trials for their control with chemicals and biocontrol agents. *Plant Disease* 102(7): 1189–1217. https://doi.org/10.1094/PDIS-08-17-1181-FE

OIV, 2026. State of the world wine sector in 2025. International Organisation of Vine and Wine, Dijon, France: 25 pp.

Posit Team. 2026. RStudio: Integrated Development Environment for R. Posit Software, PBC, Boston, Massachusetts, USA. Available at: http://www.posit.co/

Rangel-Montoya E.A., Hernández-Martínez R., 2024. Identification and pathogenicity of *Aspergillus* species associated with vine canker in Mexico. *Journal of Plant Pathology* 106: 1311–1324. https://doi.org/10.1007/s42161-024-01686-0

Samson R.A., Visagie C.M., Houbraken J., Hong S.-B., Hubka V., … Frisvad J.C., 2014. Phylogeny, identification and nomenclature of the genus *Aspergillus*. *Studies in Mycology* 78: 141–173. https://doi.org/10.1016/j.simyco.2014.07.004

Vaidya G., Lohman D.J., Meier R., 2011. SequenceMatrix: Concatenation software for the fast assembly of multi-gene datasets with character set and codon information. *Cladistics* 27: 171–180. https://doi.org/10.1111/j.1096-0031.2010.00329.x

Vitale A., Cirvilleri G., Panebianco A., Epifani F., Perrone G., Polizzi G., 2012. Molecular characterisation and pathogenicity of *Aspergillus* Sect. Nigri causing Aspergillus vine canker of table grapes in Italy. *European Journal of Plant Pathology* 132: 483–487. https://doi.org/10.1007/s10658-011-9906-z

Wickham H., 2019. Modelr: Modelling functions that work with the pipe. https://rdrr.io/cran/modelr/man/modelr-package.html

Wong T.K., Ly-Trong N., Ren H., Demotte P., Baños H., ... Minh, B. Q., 2026. IQ-TREE 3: phylogenomic inference software using complex evolutionary models. *Molecular Biology and Evolution* 43: 1–6. https://doi.org/10.1093/molbev/msag117